

1 Measurements of global and local polarization of 2 hyperons in 200 GeV isobar collisions from STAR

3 **Xingrui Gou, for the STAR Collaboration**

4 *^aInstitute of Frontier and Interdisciplinary Science & Key Laboratory of Particle Physics and Particle
5 Irradiation (Ministry of Education), Shandong University, Qingdao, Shandong, China*

6 *E-mail: Gouxr@sdu.edu.cn*

In these proceedings, we present the measurements of global polarization for Λ , $\bar{\Lambda}$ with the high-
statistics data collected by the STAR experiment for isobar (Ru+Ru, Zr+Zr) collisions at $\sqrt{s_{NN}} =$
200 GeV. These measurements allow us to study possible magnetic field driven effects through
the polarization difference and system size dependence of global polarization. Furthermore, we
7 present the first measurements of Λ , $\bar{\Lambda}$ hyperon local polarization in isobar collisions at $\sqrt{s_{NN}} =$
200 GeV. Comparisons with previous measurements in Au+Au and Pb+Pb collisions at RHIC
and LHC provide important insights into the collision system size and energy dependence of the
vorticities.

*25th International Spin Physics Symposium (SPIN 2023)
24-29 September 2023
Durham, NC, USA*

1. Introduction

In non-central heavy-ion collisions, the produced system has large orbital angular momentum and may have a strong vortical structure, which leads to the global spin polarization of hyperons through the spin-orbital interaction [1]. Due to the nature of the weak decay, Λ hyperon's polarization can be determined through the angular distribution of decay daughter proton in parent's rest frame. Global polarization has been observed for Λ and $\bar{\Lambda}$ hyperons in Au+Au collisions from $\sqrt{s_{NN}} = 3$ to 200 GeV by the STAR experiment [2].

In these proceedings, we report $\Lambda(\bar{\Lambda})$ global and local polarization as a function of centrality in Ru+Ru and Zr+Zr collisions at $\sqrt{s_{NN}} = 200$ GeV, using the data collected by STAR experiment.

2. Global polarization results

In the STAR experiment, the global polarization is determined by

$$P_{\Lambda} = \frac{8}{\alpha\pi} \frac{1}{A^0} \frac{\langle \sin(\Psi_1 - \phi_p^*) \rangle}{\text{Res}(\Psi_1)}, \quad (1)$$

where α is the decay parameter, A^0 is the acceptance correction factor, ϕ_p^* is the azimuthal angle of decay proton in Λ 's rest frame. The first order event plane (EP) direction Ψ_1 and the EP resolution $\text{Res}(\Psi_1)$ are determined using the Zero Degree Calorimeters with Shower Maximum Detectors (ZDC SMD). $\Lambda(\bar{\Lambda})$ hyperons have been reconstructed through the decay channel: $\Lambda \rightarrow \pi^- + p$ ($\bar{\Lambda} \rightarrow \pi^+ + \bar{p}$).

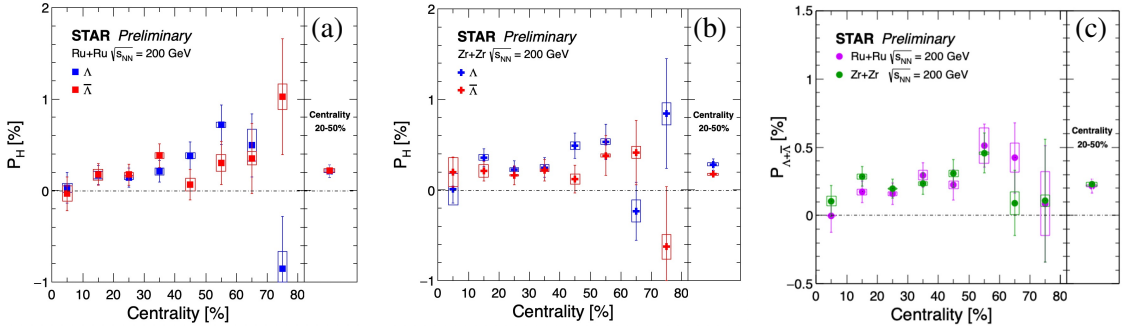


Figure 1: Global polarization of Λ and $\bar{\Lambda}$ as a function of centrality in Ru+Ru(a), Zr+Zr(b) collisions at $\sqrt{s_{NN}} = 200$ GeV. Panel (c) shows $\Lambda+\bar{\Lambda}$ global polarization results in isobar collisions. Open boxes and vertical lines represent systematic and statistical uncertainties.

Figure 1 (a) and (b) show Λ and $\bar{\Lambda}$ global polarization $P_{\Lambda, \bar{\Lambda}}$ as a function of centrality in Ru+Ru and Zr+Zr collisions. The polarization increases from central to peripheral collisions. In order to achieve a better precision in polarization splitting, we also combine measurements in 20-50% centrality. No significant difference between Λ and $\bar{\Lambda}$ global polarization in Ru+Ru and Zr+Zr collisions is observed. It indicates that there is no magnetic field driven effects on the hyperon polarization within present statistical precision. Figure 1 (c) shows $\Lambda+\bar{\Lambda}$ global polarization $P_{\Lambda+\bar{\Lambda}}$ as a function of centrality in Ru+Ru and Zr+Zr collisions. The results are consistent in each centrality between Ru+Ru and Zr+Zr collisions.

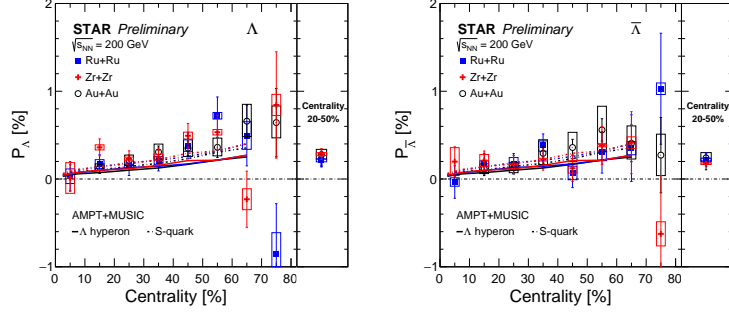


Figure 2: Λ (left) and $\bar{\Lambda}$ (right) global polarization as a function of centrality in Ru+Ru, Zr+Zr, and Au+Au collisions at $\sqrt{s_{NN}} = 200$ GeV.

32 Figure 2 shows Λ and $\bar{\Lambda}$ global polarization comparison between isobar and Au+Au collisions.
 33 The results are consistent for the whole centrality range, indicating there is no obvious collision
 34 system size dependence. The hydrodynamic model calculations from Λ polarization scenario and
 35 s -quark polarization scenario are consistent with the experiment data[3].

36 3. Local polarization results

37 The component of the polarization along the beam direction can be measured by

$$\langle \cos\theta_p^* \rangle = \int \frac{dN}{d\Omega^*} \cos\theta_p^* d\Omega^*, \quad (2)$$

38 where θ_p^* is the polar angle of the daughter proton in the Λ rest frame [4].

39 STAR has measured the local polarization with respect to the second-order event plane in
 40 Au+Au collisions at $\sqrt{s_{NN}} = 200$ GeV. The local polarization $\langle \cos\theta_p^* \rangle$ as a function of azimuthal angle
 41 relative to the second-order event plane shows a sine modulation, as expected from quadrupole
 42 structure of vorticity along the beam direction.

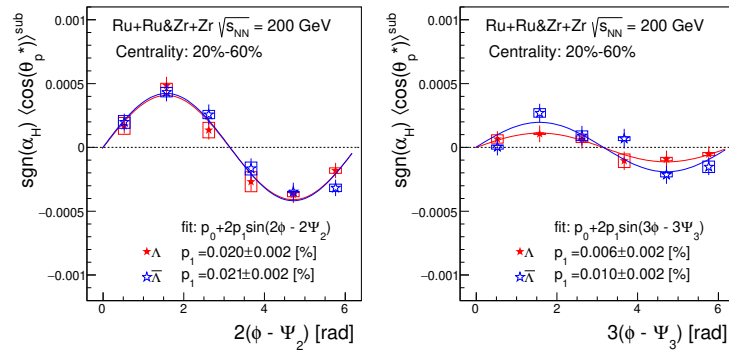


Figure 3: Local polarization $\langle \cos\theta_p^* \rangle$ of Λ and $\bar{\Lambda}$ hyperons as a function of azimuthal angle ϕ relative to the second and third-order event plane in isobar collisions at $\sqrt{s_{NN}} = 200$ GeV.

43 Figure 3 shows $\langle \cos\theta_p^* \rangle$ of Λ and $\bar{\Lambda}$ hyperons as a function of azimuthal angle ϕ relative to the
 44 second-order event plane Ψ_2 (left) and third-order event plane Ψ_3 (right) for 20% – 60% centrality,

45 respectively, in isobar collisions at $\sqrt{s_{NN}} = 200$ GeV. The second and third-order event planes are
 46 determined by the Time Projection Chamber detector (TPC). The solid lines are the fits to the results
 47 with $p_0 + 2p_1 \sin(n\phi - n\Psi_n)$. The left panel in figure 3 shows a clear sine modulation in polarization
 48 signal, as expected from quadrupole structure of vorticity along the beam direction. The pattern in
 49 isobar collisions is similar to that in Au+Au with better statistical significance. Figure 3 (right)
 50 shows the first measurements of $\langle \cos\theta_p^* \rangle$ with respect to the third-order event plane Ψ_3 . The results
 51 also show a sine modulation for both Λ and $\bar{\Lambda}$, indicating triangular flow driven polarization[5].

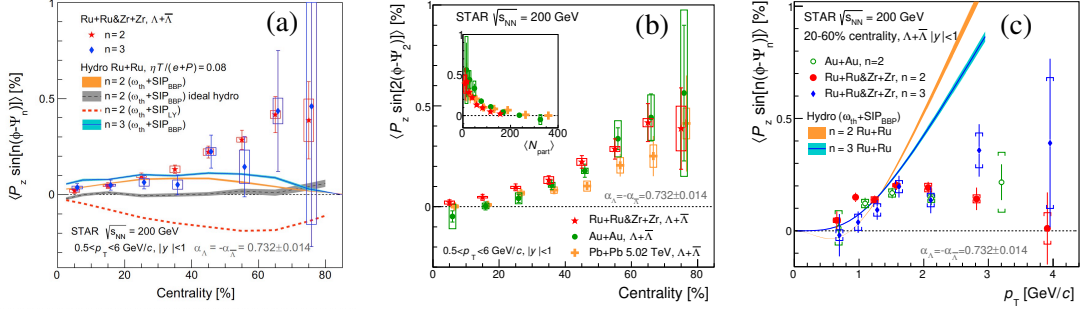


Figure 4: (a): the local polarization w.r.t 2nd(3rd) event plane of $\Lambda + \bar{\Lambda}$ as a function of the collision centrality in isobar collisions at $\sqrt{s_{NN}} = 200$ GeV. (b): the comparison of the second Fourier sine coefficient of $\Lambda + \bar{\Lambda}$ local polarization among isobar, Au+Au collisions at $\sqrt{s_{NN}} = 200$ GeV and Pb+Pb collisions at $\sqrt{s_{NN}} = 5.02$ TeV. (c): local polarization w.r.t 2nd(3rd) event plane of $\Lambda + \bar{\Lambda}$ as a function of transverse momentum.

52 Figure 4 (a) presents the comparison of centrality dependence of magnitude of $\Lambda + \bar{\Lambda}$ local polar-
 53 ization with respect to second and third EPs. The results from second order event plane increase
 54 in magnitude towards peripheral collisions, similar to the behavior of elliptic flow. The results
 55 from third order also increases from central to peripheral collisions. However, there is no signifi-
 56 cant difference between the second-order and third-order local polarization within measurement
 57 uncertainties.

58 Figure 4 (b) shows the $\Lambda + \bar{\Lambda}$ local polarization with respect to the second-order event plane as
 59 a function of the collision centrality in isobar, Au+Au, and Pb+Pb collisions[6]. A hint of system
 60 size dependence has been observed when compared isobar, Au+Au collisions at $\sqrt{s_{NN}} = 200$ GeV,
 61 while the collision energy dependence is not obvious between $\sqrt{s_{NN}} = 200$ GeV Au+Au collisions
 62 and $\sqrt{s_{NN}} = 5.02$ TeV Pb+Pb collisions.

63 The local polarization relative to both event planes are plotted as a function of hyperons' trans-
 64 verse momentum in Figure 4 (c). Results show that p_T dependence of the polarization is indeed
 65 similar to that of elliptic (v_2) and triangular (v_3) flow.

66 4. Summary

67 The global and local polarization of Λ and $\bar{\Lambda}$ have been measured in isobar (Ru+Ru, Zr+Zr)
 68 collisions at $\sqrt{s_{NN}} = 200$ GeV. The global polarization of Λ and $\bar{\Lambda}$ are consistent, indicating that the
 69 magnetic field effects on global polarization are not observed within current statistical limitation.
 70 The global polarization is consistent across collisions with different system sizes, Ru+Ru, Zr+Zr,

71 and Au+Au at same beam energy. Significant local polarization signals with respect to the second-
72 order and third-order event plane are observed in isobar collisions at $\sqrt{s_{NN}} = 200$ GeV. A slight hint
73 of collision system size dependence has been observed, while energy dependence is not obvious.

74 **Acknowledgements**

75 The author is supported by the National Key Research and Development Program of China
76 (Grant No. 2022FYA1604903)

77 **References**

- 78 [1] Z. T. Liang and X. N. Wang, Phys. Rev. Lett. 94,102301 (2005); 96, 039901(E) (2006).
79 [2] L. Adamczyk et al., (STAR Collaboration), Nature 548, 62 (2017).
80 [3] B. Fu et al, arXiv: 2201.12970 (2022).
81 [4] J. Adam et al., (STAR Collaboration), Phys. Rev. Lett. 123, 132301(2019)
82 [5] J. Adam et al., (STAR Collaboration), Phys. Rev. Lett. 131, 202301(2023)
83 [6] S. Acharya et al., (ALICE Collaboration), Phys. Rev. Lett. 128 (2022) 17, 172005.
84 [7] J. Adam et al., (STAR Collaboration), Phys.Rev.C 108 1, 014910 (2023).